

CONF-950170--1

LA-UR- 95- 211

*Title:* "Bubble Fusion": Preliminary Estimates of Spherical Micro-Implosions in Cavitating Liquids

*Author(s):* Robert A. Krakowski

*Submitted to:* DOE/EPRI Workshop on the Physics of Spherical Continuous Inertial Fusion  
Santa Fe, NM  
January 12-14, 1995

MASTER



**Los Alamos**  
NATIONAL LABORATORY

Los Alamos National Laboratory, an affirmative action/equal opportunity employer, is operated by the University of California for the U.S. Department of Energy under contract W-7405-ENG-36. By acceptance of this article, the publisher recognizes that the U.S. Government retains a nonexclusive, royalty-free license to publish or reproduce the published form of this contribution, or to allow others to do so, for U.S. Government purposes. The Los Alamos National Laboratory requests that the publisher identify this article as work performed under the auspices of the U.S. Department of Energy.

DISTRIBUTION OF THIS DOCUMENT IS UNLIMITED

35

Form No. 836 R5  
ST 2629 10/91

## **DISCLAIMER**

**Portions of this document may be illegible  
in electronic image products. Images are  
produced from the best available original  
document.**

## "BUBBLE FUSION": PRELIMINARY ESTIMATES OF SPHERICAL MICRO-IMPLOSIONS IN CAVITATING LIQUIDS

R. A. Krakowski  
Group TSA-3  
Systems Engineering and Integration Group  
January 5, 1995

### I. BACKGROUND

Liquids irradiated with intense ultrasonic waves can generate small cavities or bubbles. Upon nonlinear expansion to a state of disequilibrium, wherein the externally imposed hydrostatic pressure far exceeds that of entrapped non-condensable gas, these bubbles undergo a rapid and violent collapse. This collapse, if symmetric, can generate high pressures and temperatures through a number of possible mechanisms. The simplest and oldest explanation<sup>1,2</sup> suggests a focusing of the kinetic energy of all the surrounding liquid onto the collapsing bubble and the subsequent heating of entrapped gases under either adiabatic or isothermal conditions. Although induced by externally imposed millisecond pressure oscillations, these collapses can occur on sub-microsecond timescales and are accompanied by picosecond light emissions;<sup>3</sup> this combination of sound and light is called sonoluminescence. Recent explanations of observed high temperatures and picosecond radiation pulses accompanying such collapses are based on the interaction of multiple shock waves that are launched off the inward-moving cavity wall.<sup>4-6</sup> Other potential explanations invoke dipole emissions induced by intermolecular collisions<sup>7</sup> or the release of Casimir energy<sup>8</sup> when a dielectric hole is filled<sup>9</sup>. Conjectures have been made<sup>10-13</sup> that the processes responsible for sonoluminescence<sup>11,14,15</sup> may be extended to generated conditions where thermonuclear fusions might occur. Such an achievement would extend scientific interest in sonoluminescence out of a purely chemical context<sup>16-19</sup> to include the study of matter subjected to more extreme conditions. The main goal of this "scoping" study is to understand better conditions where deuterium-tritium fusions might be observed in conjunction with micro-implosions in cavitating liquids; prognoses of fusion application at this point are unintended.

### II. MODEL

The present "scoping" calculations are based on modeling uniform, nearly adiabatic compressional heating of a hard-sphere (van der Waals) gas in a collapsing cavity using a formalism that differs little from that reported by Lord Rayleigh nearly eighty years ago<sup>1,2</sup>. The collapse of a gas-filled bubble with an (initial) internal gas pressure,  $P_{go}$ , much less than an applied hydrostatic,  $P_h$ , was simply and accurately modeled in 1917 by Lord Rayleigh<sup>1</sup>, who suggested that the potential energy  $\sim(4/3)R_o^3(P_h - P_{go})$  created by the formation of a non-equilibrium cavity of radius  $R_o$  in a hydrostatically pressurized liquid could be converted to kinetic energy of all the surrounding liquid and focused onto the gas trapped in the cavity of ever-diminishing radius  $R(t)$ . This "disequilibrium" bubble (e.g.,  $f_{eq} = P_{go}/P_{go}^{EQ} \ll 1$ , where  $P_{go}^{EQ}$  is the gas pressure needed to achieve force balance with the environment, can be viewed as a three-dimensional "sling shot", cocked and ready to convert the elastically stored potential energy in the liquid to pressure-volume work on the contained gas.

When a time-varying pressure,  $P_a(t)$ , is added to the hydrostatic pressure,  $P_h$ , far from the bubble and included in the balance between kinetic energy, potential energy, and work, along with the addition of a viscous pressure term<sup>13</sup>  $[\sim 4 \eta R^2 (dR/dt)/r]$  to  $P_h$ , and using pressure balance, the following (Rayleigh-Plesset) bubble-dynamics equation results:

$$\rho_\ell \left[ R \frac{dv}{dt} + \frac{3}{2} v^2 \right] = (P_h + P_{\sigma 0} - P_v) z^\gamma + P_v z^{1/3} - \frac{4 \eta v z^{1/3}}{R_0} - P_h - P_a(t) , \quad (1)$$

where  $v = dR/dt$ ,  $z = (R_0/R)^3 = 1/x^3$ ,  $\rho_\ell$  is the liquid density,  $P_{\sigma 0} = 2 \sigma/R_0$  is the Laplace or surface tension pressure, and  $\eta$  is the liquid-phase viscosity (assumed in these computations to be zero). The Rayleigh-Plesset (Noltingk-Neppiras-Poritsky)<sup>2</sup> equation describes a highly idealized bubble and is subject to a number of important limitation, some of which are listed below<sup>2,14,16</sup>:

- single bubble in an infinite medium
- spherical bubble, no distortions or breakup
- spatially uniformity within and outside the bubble
- absence of body forces
- acoustic wavelengths (associated with  $P_a$ ) much greater than  $R$
- no viscous effects within the bulk liquid [the viscous term in Eqn. (1) is associated only with fluid motion near the bubble surface]
- incompressible liquid phase
- constant gas inventory within the bubble
- constant liquid vapor pressure (isothermal cavity wall)
- no molecular diffusion into or out of the bubble
- no acoustic streaming and impact of resulting shear stresses on bubble shape
- ideal-gas, adiabatic behavior within the bubble with a constant polytropic index.
- no radiation loss from the gas/plasma within the bubble
- no gas-phase shock formation (e.g., gas-phase speed of sound,  $c >> dR/dt$ ).

Within these limitations, Eqn. (1) is solved for both a range of harmonic and aharmonic/resonant pressure functions, starting with an equilibrium bubble ( $x = R_0/R_0^{EQ} = 1$ ,  $f_{eq} = 1$ ). In the case of driven systems, an initial radius,  $R_0^{EQ}$ , is chosen to give a natural resonant frequency,  $\omega_r = \sqrt{P_h/\rho_\ell} / R_0$ , equal to the driver frequency,  $2\pi f$ ; otherwise, a significant part of the numerical computation is devoted to resolving uninteresting transient effects<sup>23</sup>. In addition to determining  $R(t)$  and  $T(t)$ , the resulting gas pressure,  $P_g(t)$ , is

assumed to be generated in a deuterium- tritium (DT) gas mixture, an impulse parameter  $\int P_g dt \sim \langle n \tau T \rangle$

is computed for each compression the arises, and the DT fusion yield per compression,  $YLD$ , for each compression registered. These integral quantities, along with the peak radial compression,  $x_{min} = R_{min}/R_0$ , and the maximum temperature,  $T(x_{min})$ , are correlated with the disequilibrium parameter,  $f_{eq} = P_{go}/P_{go}^{EQ}$ , evaluated at the beginning of each major compression. Both DT depletion through burnup and fusion-product heating are monitored, but this information is not incorporated into the time-dependent model; for most of the conditions examined, these fusion-related effects on the bubble dynamics and response are not important. In addition to the use of a van der Waals equation of state, a second correction to the ideal-gas adiabat is applied to adjust (approximately) for "sliding adiabaticity" associated with energy shed from the compressing bubble in the form of free-free electron (Bremsstrahlung) radiation. The degree of ionization

is assumed to be given by the Saha equilibrium relationship<sup>21,22</sup>. The dissociation of DT is neglected, and the atomic and ionic partition functions are taken as unity.

The analysis reported herein parametrically describes in a fusion context (e.g., fusion neutron yield, density-time-temperature product) the effect of varying the loading of this three-dimensional “sling shot” *vis à vis* the disequilibrium parameter  $f_{eq}$ . Equation (1) is solved with  $P_g = f_{eq}P_{go}$  at  $t = 0$  and  $P_a(t) = 0$  to model the “Rayleigh collapse”, peak parameters, and integrated fusion parameters (e.g.,  $\langle n \tau T \rangle$  and YLD) as a function of  $f_{eq}$ ; the mechanism and trajectory by which this level of disequilibrium is achieved is not modeled here. The feasibility of achieving the required level of disequilibrium starting with an equilibrium bubble (e.g.,  $f_{eq} = 1$ ) is investigated and reported elsewhere<sup>20</sup> by solving the Rayleigh-Plesset equation under conditions of both harmonic and aharmonic/resonant pressure loadings of the liquid surrounding the (initially) equilibrium bubble; for reasons of space, only the parametric variation of  $f_{eq}$  is reported here.

### III. RESULTS

The “disequilibrium” parameter  $f_{eq}$  along with and initial equilibrium bubble radius,  $R_o^{EQ}$ , are specified to determine an initial normalized (disequilibrium) radius,  $x_o = R_o/R_o^{EQ}$ , with which to begin the time-dependent calculation of  $R(t)$  and the fusion-related integral and peak parameters. Figure 1 gives a schematic representation of the case wherein an equilibrium ( $x = 1$ ,  $f_{eq} = 1$ ) bubble is brought by some unspecified route to a state of disequilibrium ( $f_{eq} < 1$ ), the resulting three-dimensional “sling shot” is released, and the ensuing compression (and rebound) is numerically followed in time by means of Eqn. (1). The unspecified (unmodeled) equilibrium  $\rightarrow$  disequilibrium trajectory,  $x = 1 \rightarrow x_o$  is assumed to occur slowly (relative to the time scale of the ensuing collapse) and isothermally. All computations that vary  $f_{eq}$  parametrically correspond to an equilibrium bubble of radius  $R_o^{EQ} = 100 \mu\text{m}$ , with the isothermal excursion to the initial radius  $R_o$ , where actual modeling of the bubble collapse begins, being given by  $x_o = [1/f_{eq} + v_H^*]/(1 + v_H^*)^{1/3}$ . In this expression,  $x_o = R_o/R_o^{EQ}$  and  $\rho_o = (P_h + P_{\sigma o} - P_{vo})/(R_G T_o)$  is the DT gas density in the equilibrium ( $x = 1$ ) bubble and  $v_H^* = \rho_o v_H$ , where  $v_H$  is the van der Waals hard-sphere volume; for all cases reported, with  $P_h = 1 \times 10^5 \text{ Pa}$  and  $P_{\sigma o} = 2 \sigma/R_o^{EQ}$ .

The parametric dependencies of  $x_{min}/x_o = R_{min}/R_o$ ,  $\langle n\tau T \rangle/10^6$ , YLD/10<sup>6</sup>, and  $T(x_{min})$  on  $f_{eq}$  are shown on Fig. 2. The sample normalized-radius trajectory (during compression) used in the Fig.-1 illustration corresponds to  $f_{eq} = 0.01$ . Shown also is the  $f_{eq}$  dependence of  $x_{min} = R_{min}/R_o^{EQ}$ . The peak temperatures reported correspond to an adiabatic heating along that starts with a disequilibrium bubble at  $T_o = 300 \text{ K}$ , under the assumption that the equilibrium  $\rightarrow$  disequilibrium trajectory was achieved slowly and isothermally. Shown also on Fig. 2 are peak temperatures for the case where the expansion part of the trajectory was also adiabatic. The  $\langle n\tau T \rangle$  and YLD values reported on Fig. 2, however, correspond to the more optimistic isothermal equilibrium  $\rightarrow$  disequilibrium trajectory. For this case, measurable quantities of neutrons from a single bubble collapse would require that bubble to be “set up” with  $f_{eq} < 10^{-4}$ . Considerably lower (more-demanding) values of  $f_{eq}$  would be required if the assumed expansion from the equilibrium to the disequilibrium state (Fig. 1) is adiabatic<sup>20</sup>. Examples are given in Ref. 20 of means to achieve the required  $f_{eq}$  values by exciting an (initially) equilibrium bubble with strong acoustic waves, but non-adiabatic expansion (e.g., expansion without cooling) are needed for measurable fusion yields (per compression) to be predicted.

An estimate of the efficiency with which fusion might be generated can be made using the system described in Fig. 3. The fusion power that might be generated from a system of  $n_B(1/\text{m}^3)$  bubbles per unit volume

being irradiated with acoustic energy of amplitude  $P_A$ (MPa) and frequency  $f$ (Hz) is measured as the ratio  $Q_F$  relative to the acoustic power,  $P_A^2/(2Z_\ell)/Q_A(10^6 \text{MW/m}^2)$ , where  $Q_A$  is given on Fig. 3 as the acoustic-energy Q-value in terms of the pressure-amplitude reflection coefficient,  $R$ , and  $Z_\ell \leq c_\ell \rho_\ell$  is the acoustic impedance of the liquid; for a combination of room-temperature water and most metals,  $Q_A = 3-5$ . The maximum density of active bubbles,  $n_B$ , is dictated by the minimum volume of liquid surrounding each active (disequilibrium) bubble needed to contribute to the collapse, as measured here by the ratio  $(r_c/R_o)_{\min}$ . Hence, with  $R_o$  and  $R_o^{\text{EQ}}$  being the (maximum) disequilibrium and equilibrium bubble radii, respectively, and the volume of the equilibrium bubble being designated as  $V_o^{\text{EQ}} = (4/3)\pi(R_o^{\text{EQ}})^3$ , the density of active bubbles conservatively is given by  $f_{\text{eq}}/V_o^{\text{EQ}}/(r_c/R_o)^3_{\min}$ . With these definitions, the following relationships for  $Q_F$  and the average fusion power density,  $[\text{PD}]_F(\text{MW/m}^3)$ , result:

$$\frac{Q_F}{LQ_A} < \frac{2 \times 10^{-6} c_\ell}{(P_A / \rho_\ell)^2} \frac{f_{\text{eq}}}{(r_c / R_o)^3_{\min}} \frac{[\text{YLD}]E_f e (f / N)}{V_o^{\text{EQ}} \rho_\ell} . \quad (2)$$

$$[\text{PD}]_F(\text{MW/m}^3) = [\text{YLD}]E_f e (f / N) n_B . \quad (3)$$

In these expressions, the drive frequency is  $f$ , and the subharmonic collapse occurs  $1/N$  acoustic cycles ( $N \sim 4$  for the  $f = 10$  kHz case reported in Ref 20). The relationship between  $f_{\text{eq}}$  and  $[\text{YLD}]$  must be derived from some model, as reported for example in Fig. 2. For  $P_A = 0.1$  MPa,  $c_\ell = 1,480$  m/s,  $\rho_\ell = 1,000$  kg/m $^3$ ,  $f/N = 10^4/4$ ,  $E_f = 17.6$  MeV/(DT)fusion, and  $R_o^{\text{EQ}} = 10^{-4}$  m,

$$\frac{Q_F}{LQ_A} < 0.50 \frac{f_{\text{eq}} [\text{YLD}]}{(r_c / R_o)^3_{\min}} . \quad (4)$$

From Fig. 2,  $[\text{YLD}] \sim 10^7$  fusions/pulse when  $f_{\text{eq}} \sim 10^{-5}$ ; for  $L = 1$  m and  $Q_A = 5$ , a value of  $(r_c/R_o)_{\min} = 6.3$  would give a  $Q_F = 1$  "physics breakeven"; the (active) bubble density and the (average) fusion power for this case are  $n_B = 9,600$  bubbles/m $^3$  and  $[\text{PD}]_F = 6.7 \times 10^{-4}$  MW/m $^3$ . The scaling relationship suggested in Eqn. (4) indicates a number of routes to improved performance:

- increased acoustic Q-value,  $Q_A$
- increased fusion yield,  $[\text{YLD}]$ (fusions/pulse), for less disequilibrium, (e.g., increased  $f_{\text{eq}}$ ) and reduced (initial, equilibrium) bubble radius,  $R_o^{\text{EQ}}$ .
- reduced acoustic drive,  $P_A$ , without compromising the two items listed above.
- reduced unit-cell volume per active bubble (e.g., increased  $n_B$  and improved utilization of the invested acoustic energy), as measured by  $(r_c/R_o)^3_{\min}$ ; essentially, more of the liquid mass would be used (e.g., "shared") to provide inertial drive to more than one active bubble.

#### IV. CONCLUSIONS

Results of analyses based on a simplified model<sup>20</sup> are reported herein indicate the potential of observing thermonuclear fusion in a collapsing gas-filled bubble. This conclusion is made on the basis of the modelistic limitations listed above and the ability to achieve large disequilibria (e.g.,  $f_{\text{eq}} < 10^{-4} - 10^{-5}$ ) along a stable and reasonably isothermal<sup>13</sup> trajectory. A program to improve the reliability of these projections

requires both a properly directed and diagnosed experiment as well as more detailed and realistic numerical simulations. It seems appropriate to launch a small effort to understand and possibly to enhance the micro-implosions responsible for sonoluminescence and possibly "sono-fusion". The attributes of such a program include:

- offers an inexpensive opportunity for a "long-shot" demonstration of thermonuclear fusion, with possible support of existing or planned devices and diagnostics for the study of Inertial-Confinement Fusion.
- presents a means to advance understanding of chemical and atomic processes related to reactive shocks, collision-induced dipole emission<sup>7</sup>, and gas-dynamic lasing<sup>13,23</sup>.
- permits application, modification, extension, and development of diagnostics for use in resolving the spatial and radiative dynamics of fast micro-implosions.
- provides an inexpensive experimental means for benchmarking hydrodynamics and plasma simulation models and the physical-properties data base they use.
- contributes chemical and atomic-physics understanding of an area that is far from resolved, is of high current interest, and could lead to new chemical processing schemes, including in situ chemical modification of a range of stored waste.

The simplified simulation model used here and in Ref. 20 must be extended to include: a) multiple, interacting shock waves<sup>4-6</sup>; b) gradient-driven transport phenomena; c) gas/plasma-(cavity)wall interactions; d) improved physical- properties data base, including that use to model the fusion physics.

## REFERENCES

1. Lord Rayleigh, "On the Pressure Development in a Liquid During the Collapse of a Spherical Cavity," *Phil. Mag.*, **34**(6), 94 (1917).
2. T. J. Leighton, **The Acoustic Bubble**, Academic Press Limited, London (1994).
3. B. P. Barber and S. J. Puttermann, "Observation of Synchronous Picosecond Sonoluminescence," *Nature*, **352**, 318 (July 25, 1991).
4. H. P. Greenspan and A. Nadim, "On sonoluminescence of an Oscillating Gas Bubble," *Phys. Fluids*, **A5**(4), 1065 (1993).
5. C. C. Wu and P. H. Roberts, "Shock-Wave Propagation in a Sonoluminescing Gas Bubble," *Phys. Rev. Lett.*, **70**(22), 3424 (1993).
6. C. C. Wu and P. H. Roberts, "A Model of Sonoluminescence," *Proc. R. Soc., London*, **445**, 323 (1994).
7. L. Frommhold and A. A. Atchley, "Is Sonoluminescence due to Collision- Induced Emission?," *Phys. Rev. Lett.*, **73**(21), 2883 (1994).
8. M. Krich, **The Casimir Effect in Critical Systems**, World Scientific Publishers, Singapore, (1994).
9. J. Schwinger, "Casimir Light: The Source," *Proc. Natl. Acad. Sci.*, **90**, 2105 (1993).
10. M. A. Margulies, "Modern Views on the Nature of Acousto-chemical Reactions," *Russ. J. Phys. Chem.*, **50**, 1 (January 1976) [translated from *Zhurnal Fizicheskoi Khimii*, **50**, 1-18 (1976)].
11. L. A. Crum, "Sonoluminescence," *Physics Today*, p. 22, (September 1994).
12. B.P. Barber, C. C. Wu, R. Loefstedt, P. H. Roberts, and S. J. Puttermann, "Sensitivity of Sonoluminescence to Experimental Parameters," *Phys. Rev. Lett.*, **72**(9), 1380 (1994).
13. T. V. Prevenslik, "Sonoluminescence Induced Deuterium Fusion," *Trans. Fusion Technology* **26**(12), 530 (1994).
14. K. S. Suslick, "The Chemical Effects of Ultrasound," *Scientific American*, p. 80 (February 1989).
15. L. A. Crum and R. A. Roy, "Sonoluminescence," *Science*, **266**, 233 (1994).
16. T. J. Mason and J. P. Lorimer, **Sonochemistry: Theory, Applications and Uses of Ultrasound in Chemistry**, Ellis Horwood Limited, Chichester UK (1984).
17. K. S. Suslick, **Ultrasound: Its Chemical, Physical, and Biological Effects**, VCH Publishers, Weinheim, Germany (1988).

18. Sonochemistry Special Issue, Ultrasonics, 30(3) (1992).
19. M. A. Margulis, "Fundamental Aspects of Sonochemistry," Ultrasonics, 30(3), 4 (1992).
20. R. A. Krakowski, "Bubble Fusion: Preliminary Estimates," Los Alamos National Laboratory document LA-UR-95-100 (January 12, 1995).
21. Ya. B. Zel'dovich and Yu. P. Raizer, **Physics of Shock Waves and High-Temperature Hydrodynamic Phenomena**, Academic Press, N.Y. (1966).
22. M. I. Boulos, P. Fauchais, and E. Pfender, **Thermal Plasmas: Fundamentals and Applications**, Plenum Press, N.Y. (1994).
23. I. R. Hurle and A. Hertzberg, "Electronic Population Inversion by Fluid-Mechanical Techniques," Phys. Fluids, 8(9), 1601 (1965).

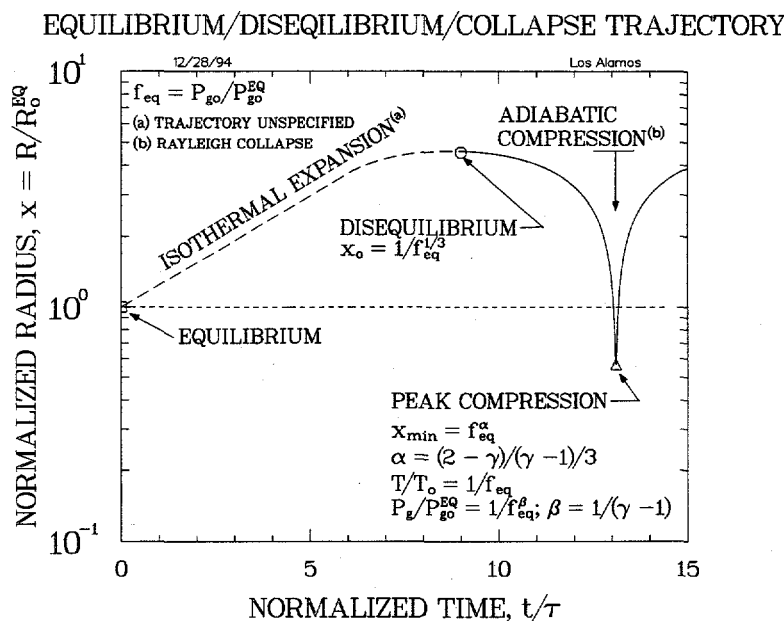


Figure 1. Schematic diagram of bubble radius trajectory illustrating approach to  $f_{eq} < 1$  disequilibrium from  $f_{eq}$ ,  $x = 1$  equilibrium state, followed by collapse to  $x_{min}$ .

## DISCLAIMER

This report was prepared as an account of work sponsored by an agency of the United States Government. Neither the United States Government nor any agency thereof, nor any of their employees, makes any warranty, express or implied, or assumes any legal liability or responsibility for the accuracy, completeness, or usefulness of any information, apparatus, product, or process disclosed, or represents that its use would not infringe privately owned rights. Reference herein to any specific commercial product, process, or service by trade name, trademark, manufacturer, or otherwise does not necessarily constitute or imply its endorsement, recommendation, or favoring by the United States Government or any agency thereof. The views and opinions of authors expressed herein do not necessarily state or reflect those of the United States Government or any agency thereof.

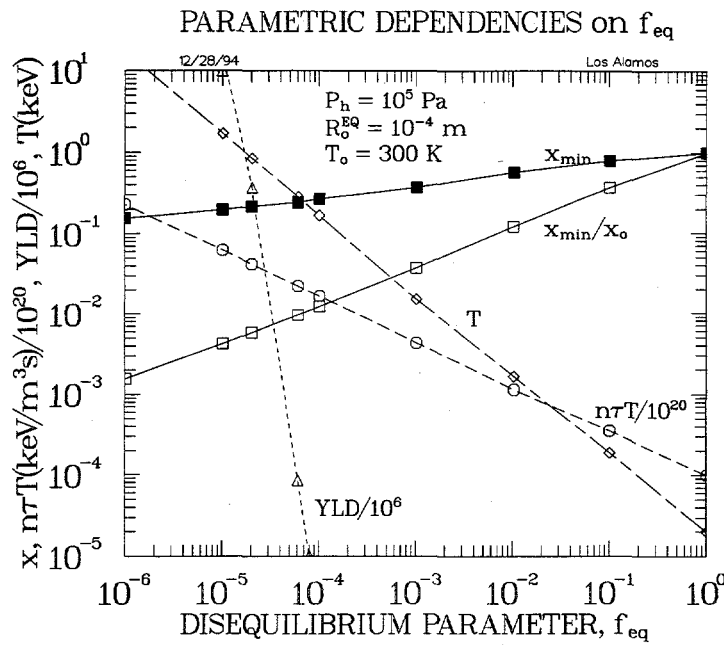


Figure 2. Parametric dependence of integral and peak-compression parameters on disequilibrium parameter,  $f_{eq} = P_{go}/P_{go}^{EQ}$ , under assumption of isothermal expansion prior to adiabatic collapse to peak temperature  $T$ .

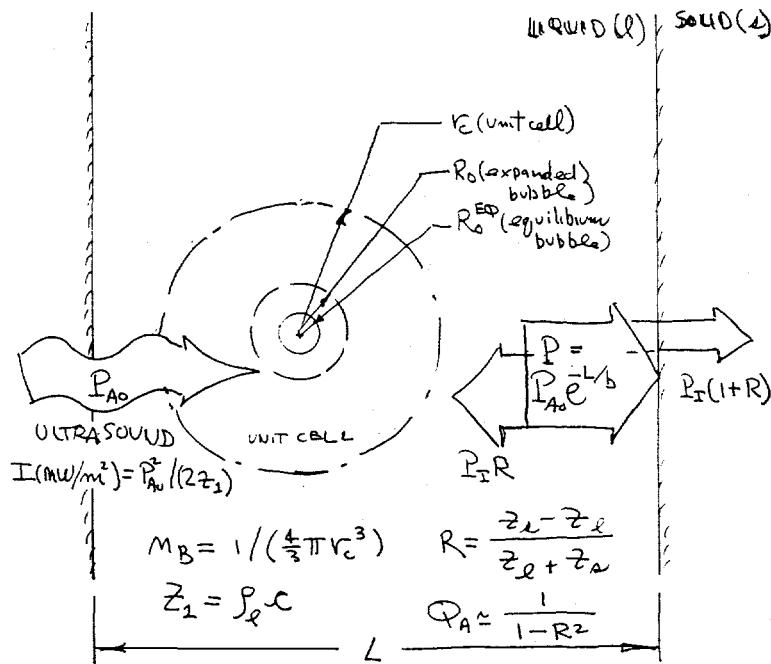


Figure 3. Schematic of system used to estimate fusion Q-value,  $Q_F = [\text{Fusion Power}]/[\text{Acoustic Power}]$ , where [Fusion Power] ( $\text{MW/m}^2$ ) =  $[\text{YLD}]E_F e (f/N) n_B L$  and [Acoustic Power] ( $\text{MW/m}^2$ ) =  $P_A^2/(2Z_\ell)/Q_A$ . The pressure-amplitude reflection coefficient is  $R$ , and the acoustic impedances,  $Z_{\ell,s}$ , or the liquid and solid, respectively<sup>2</sup>.